



AFRL-RY-WP-TP-2009-1327

**PROGRESS IN ORIENTATION-PATTERNED GaAs FOR
NEXT-GENERATION NONLINEAR OPTICAL DEVICES
(Postprint)**

Rita D. Peterson, David Bliss, Candace Lynch, and David H. Tomich

**Electro-Optical Countermeasures Technology Branch
Electro-Optical Sensor Technology Division**

**FEBRUARY 2008
Final Report**

Approved for public release; distribution unlimited.

See additional restrictions described on inside pages

STINFO COPY

**AIR FORCE RESEARCH LABORATORY
SENSORS DIRECTORATE
WRIGHT-PATTERSON AIR FORCE BASE, OH 45433-7320
AIR FORCE MATERIEL COMMAND
UNITED STATES AIR FORCE**

REPORT DOCUMENTATION PAGE

Form Approved
OMB No. 0704-0188

The public reporting burden for this collection of information is estimated to average 1 hour per response, including the time for reviewing instructions, searching existing data sources, gathering and maintaining the data needed, and completing and reviewing the collection of information. Send comments regarding this burden estimate or any other aspect of this collection of information, including suggestions for reducing this burden, to Department of Defense, Washington Headquarters Services, Directorate for Information Operations and Reports (0704-0188), 1215 Jefferson Davis Highway, Suite 1204, Arlington, VA 22202-4302. Respondents should be aware that notwithstanding any other provision of law, no person shall be subject to any penalty for failing to comply with a collection of information if it does not display a currently valid OMB control number. **PLEASE DO NOT RETURN YOUR FORM TO THE ABOVE ADDRESS.**

1. REPORT DATE (DD-MM-YY) February 2008		2. REPORT TYPE Journal Article Postprint		3. DATES COVERED (From - To) 01 October 2006 – 31 January 2008	
4. TITLE AND SUBTITLE PROGRESS IN ORIENTATION-PATTERNED GAAS FOR NEXT-GENERATION NONLINEAR OPTICAL DEVICES (Postprint)				5a. CONTRACT NUMBER	
				5b. GRANT NUMBER In House	
				5c. PROGRAM ELEMENT NUMBER 62204F	
6. AUTHOR(S) Rita D. Peterson (AFRL/RYPJW) David Bliss and Candace Lynch (AFRL/RYPHC) David H. Tomich (AFRL/RXPMS)				5d. PROJECT NUMBER 2003	
				5e. TASK NUMBER 12	
				5f. WORK UNIT NUMBER 20031225	
7. PERFORMING ORGANIZATION NAME(S) AND ADDRESS(ES) Electro-Optical Countermeasures Technology Branch (AFRL/RYPJW) Electro-Optical Sensor Technology Division Air Force Research Laboratory Sensors Directorate Wright-Patterson Air Force Base OH 45433-7320				8. PERFORMING ORGANIZATION REPORT NUMBER AFRL-RY-WP-TP-2009-1327	
Electromagnetics Technology Division, Optoelectronic Technology Branch (AFRL/RYPHC) ----- Electronic & Optical Materials Branch, Materials Synthesis Section (AFRL/RXPMS) Air Force Research Laboratory, Materials and Manufacturing Directorate					
9. SPONSORING/MONITORING AGENCY NAME(S) AND ADDRESS(ES) Air Force Research Laboratory Sensors Directorate Wright-Patterson Air Force Base, OH 45433-7320 Air Force Materiel Command United States Air Force				10. SPONSORING/MONITORING AGENCY ACRONYM(S) AFRL/RYPJW	
				11. SPONSORING/MONITORING AGENCY REPORT NUMBER(S) AFRL-RY-WP-TP-2009-1327	
12. DISTRIBUTION/AVAILABILITY STATEMENT Approved for public release; distribution unlimited.					
13. SUPPLEMENTARY NOTES PAO case number WPAFB-098-0038; cleared 09 January 2008. This is a work of the U.S. Government and is not subject to copyright protection in the United States. Paper contains color.					
14. ABSTRACT Orientation-patterned GaAs (OPGaAs) shows great promise as a nonlinear optical material for frequency conversion in the 2-5 μm and 8-12 μm regions. We report recent progress in each of the three main areas of OPGaAs development: fabrication of patterned templates using a combination of wafer bonding and MBE techniques; thick-layer HVPE growth; and material and OPO device characterization. This work has led to significant improvements in material quality, specifically reduced optical loss, increased sample thickness, improved patterned domain fidelity, and greater material uniformity. Advances in material quality have in turn enabled demonstration of OPO devices operating in the 3-5 μm spectral region. Optical loss and OPO performance measurements on a series of OPGaAs samples are presented, with the goal of understanding how these properties are influenced by growth conditions, and how OPO performance may be improved. Research continues on understanding loss mechanisms, correlating performance with material properties, transitioning the technology into an industrial process, and extending it to additional materials.					
15. SUBJECT TERMS nonlinear optics, optical parametrical processes, quasi-phasesmatching, GaAs epitaxy					
16. SECURITY CLASSIFICATION OF:			17. LIMITATION OF ABSTRACT: SAR	18. NUMBER OF PAGES 18	19a. NAME OF RESPONSIBLE PERSON (Monitor) Rita D. Peterson 19b. TELEPHONE NUMBER (Include Area Code) N/A
a. REPORT Unclassified	b. ABSTRACT Unclassified	c. THIS PAGE Unclassified			

Progress in orientation-patterned GaAs for next-generation nonlinear optical devices

Rita D. Peterson^{*a}, David Bliss^b, Candace Lynch^b, David H. Tomich^c

^aAir Force Research Laboratory, AFRL/RJW, WPAFB OH 45433

^bAir Force Research Laboratory, AFRL/RJHC, Hanscom AFB, MA 01731

^cAir Force Research Laboratory, AFRL/RXPSM, WPAFB OH 45433

ABSTRACT

Orientation-patterned GaAs (OPGaAs) shows great promise as a nonlinear optical material for frequency conversion in the 2-5 μm and 8-12 μm regions. We report recent progress in each of the three main areas of OPGaAs development: fabrication of patterned templates using a combination of wafer bonding and MBE techniques; thick-layer HVPE growth; and material and OPO device characterization. This work has led to significant improvements in material quality, specifically reduced optical loss, increased sample thickness, improved patterned domain fidelity, and greater material uniformity. Advances in material quality have in turn enabled demonstration of OPO devices operating in the 3-5 μm spectral region. Optical loss and OPO performance measurements on a series of OPGaAs samples are presented, with the goal of understanding how these properties are influenced by growth conditions, and how OPO performance may be improved. Research continues on understanding loss mechanisms, correlating performance with material properties, transitioning the technology into an industrial process, and extending it to additional materials.

Keywords: orientation-patterning, quasi-phase-matching, GaAs epitaxy, nonlinear optical frequency conversion, optical parametric amplification

1. INTRODUCTION

Orientation-patterned GaAs (OPGaAs) is of interest for a variety of military and commercial applications requiring tunable radiation in the 2-5 μm and the 8-12 μm atmospheric transmission regions. Since few lasers exist which emit directly in these spectral regions, nonlinear frequency conversion techniques are generally used to convert the more readily available laser wavelengths into the longer wavelength regions of interest. OPGaAs provides nonlinear frequency conversion that can be customized across its broad transparency range by using quasi-phasematching (QPM) with a properly designed periodic structure.

Development of nonlinear frequency conversion devices for IRCM has progressed from those based on birefringently phasematched crystals like AgGaSe₂, ZnGeP₂, and KTP, to the more recent quasi-phasematched periodically poled lithium niobate (PPLN) and similar poled ferroelectrics. To reap the benefits of quasi-phasematching across the 2-5 μm and 8-12 μm regions where poled ferroelectrics are limited by intrinsic absorption, we are developing the next generation of nonlinear optical devices, based upon GaAs and similar zincblende-structure semiconductor materials.

*rita.peterson@wpafb.af.mil; phone 937-904-9657

The advantages of GaAs are well known. It is transparent from 1-12 μm , has a high nonlinear coefficient ($d_{14} \approx 90 \text{ pm/V}$), and like all quasi-phases-matched materials, can be fabricated to obtain a desired output wavelength from an available pump source. In fact, since GaAs (crystal structure $\bar{4}3m$) is isotropic in refractive index, quasi-phases-matching is the only way to take advantage of its nonlinear potential. Since it is not ferroelectric and thus cannot be poled, however, the main challenge in its development has been finding a workable method of creating the necessary $\sim 100\text{-}\mu\text{m}$ periodic structure in the material.

The earliest reported attempt to demonstrate QPM in GaAs used GaAs plates polished to an appropriate thickness and arranged at Brewster's angle, with every other plate rotated to obtain the needed inversion¹. Not surprisingly, the interaction length was limited and losses were very high. A later and more sophisticated approach involved manual assembly of a stack of polished GaAs pieces with alternating orientations, which was then diffusion bonded to reduce losses at the interfaces.² QPM frequency doubling of a CO_2 laser was demonstrated, but the process was prohibitively labor intensive, and clearly could not produce the interaction lengths and tolerances necessary to reach OPO thresholds. Finally, the now-familiar fabrication process was developed, consisting of thick-layer growth by hydride vapor phase epitaxy (HVPE) on a patterned template prepared using molecular beam epitaxy (MBE) and conventional photolithographic techniques.³ Use of a vicinal GaAs substrate polished 4° off (001) toward (111)B in combination with a nonpolar Ge buffer layer enables growth of subsequent GaAs layers with an inverted orientation relative to the substrate.

Since the original demonstration of this method, significant advances have been made in each step of the process. Template fabrication techniques based upon wafer bonding are being developed that would eliminate the need for MBE growth of a Ge layer, simplify the process, and make it more readily extended to other materials. Refinement of HVPE growth conditions has dramatically reduced material loss while increasing thickness and domain fidelity. Finally, improvement of material quality has led to a variety of frequency conversion demonstrations. Schunemann, et. al., for example, obtained almost 0.5 W of combined signal and idler output from an OPGaAs OPO operating at 3.4 and 5.2 μm with 20% slope efficiency using a Tm,Ho:YLF laser as the pump source. The output wavelength was tuned over a range of 0.5 μm by varying the OPGaAs crystal temperature.⁴ Vodopyanov, et. al. tuned an OPGaAs OPO over a wavelength range of several microns by using a combination of temperature tuning and pumping with a tunable PPLN OPO.⁵

2. TEMPLATE FABRICATION

MBE-grown templates have been available for several years now, and their quality and consistency have become sufficient for the production of numerous device-quality OPGaAs samples. Although template fabrication might seem almost routine, there are aspects of the current process that could clearly be improved upon. The most obvious issue is the need for a Ge buffer layer to force inverted growth of subsequent GaAs layers. Ge acts as a contaminant in GaAs grown for electronics applications, resulting in severe performance degradation. This means that the OPGaAs Ge layer must be grown in a separate MBE machine, or in a machine modified with an auxiliary chamber to prevent contamination of subsequent GaAs growth. Either workaround increases complexity and cost. Moreover, the need for a buffer layer limits extension of the OP technique to materials for which a suitable buffer material can be found.

To address these disadvantages, we are investigating wafer bonding techniques for template fabrication. Wafer bonding proved impractical for assembling finished samples because of the number of layers required and the interface losses, but a template needs only two layers, and laser light will not be propagated through the single bonded interface. No buffer layer is required, and although MBE growth is still used, fewer layers are needed, reducing cost and fabrication time.

The process begins with deposition of epitaxial GaAs layers onto purchased GaAs substrates to optimize surface chemistry and topography for optimum bonding uniformity. Etch stop layers are also incorporated into the epitaxial structures to facilitate material removal following the bonding step. The two layers are then rotated with respect to each other and bonded, with the bond taking place between the two epitaxial layers. Bonding is typically done under vacuum, at a temperature of 600C and an applied pressure of 35 psi. The top substrate is then ground off, exposing the bonded layers for photolithographic patterning and subsequent MBE regrowth. This process is illustrated in Figure 1.

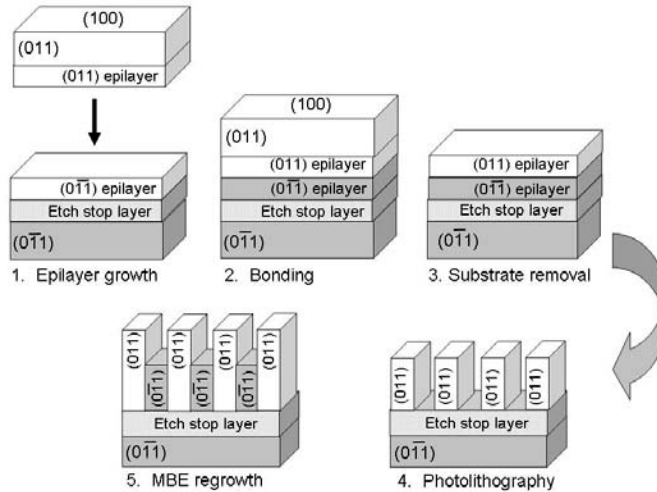


Figure 1. Template fabrication by wafer bonding.

Initial experiments have produced wafer pairs that are well bonded in the center, but poorly bonded toward the edges. Bonding was attempted first on 2-cm x 2-cm squares of GaAs, but the cut edges could not be made clean and smooth enough for a good bond, and subsequent trials have used whole 2-inch diameter wafers. Improvement in the uniformity of applied pressure has increased the size of the well bonded area, but we are still far from a completely bonded template. The photographs in Figure 2, made under infrared illumination, compare an early bonded wafer pair with a more recent one. The lighter region in the center of each picture corresponds to the well-bonded area. Fringing is apparent outside of these areas where the wafers are not completely bonded. It is encouraging that researchers at the University of Massachusetts, using a somewhat different procedure, have recently produced a bonded template on which device-quality HVPE OPGaAs has been grown.⁶

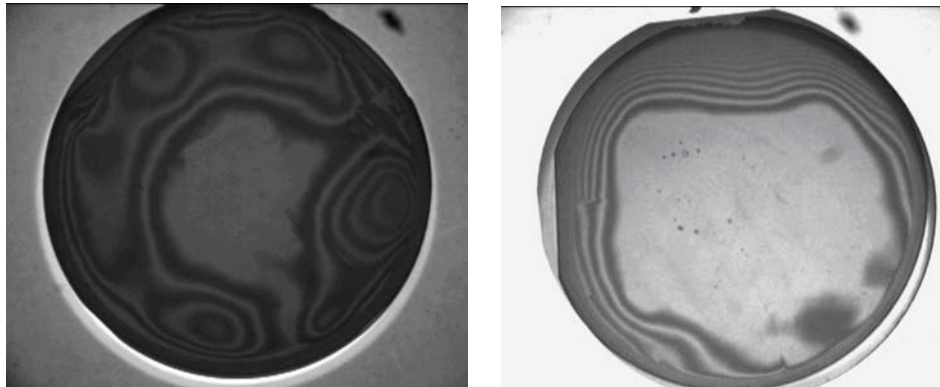


Figure 2. Examples of early (left) and more recent (right) bonded GaAs wafer pairs.

3. THICK-LAYER HVPE GROWTH

Although template quality is critical in establishing the inverted domain pattern in the finished sample, the material in which the nonlinear interaction takes place is the thick layer grown through HVPE. The first HVPE OPGaAs material was produced in France, on templates from Stanford University.⁷ After successful proof-of-concept experiments, AFRL initiated an in-house basic research program to establish a low-pressure HVPE growth capability for OP materials.⁸

Almost all of this HVPE work to date has been done on templates fabricated using Stanford’s original all-MBE process, since templates made using the wafer bonding techniques described above are just starting to become available.

There have been three main challenges in producing device-quality material: growing a layer thick enough to accommodate reasonable pump spot sizes; preserving the integrity of the QPM structure over the entire thickness; and reducing optical loss to the point where efficient frequency conversion can occur. Early samples were limited to several hundred microns of useable thickness due to the merging of domains as growth progressed (Figure 3) or the cessation of growth altogether due to parasitic growth on the inside walls of the furnace. In an initial approach to the parasitic growth problem, the sample was removed from the furnace when growth slowed, and was polished down to expose material with the proper pattern. The furnace was cleaned, and the polished sample was then put back in for further growth. Some device-quality samples were produced using this method, but it left an observable transition between the two growth stages (Figure 4), and patterned growth in the second growth stage generally terminated much more quickly than in the first.

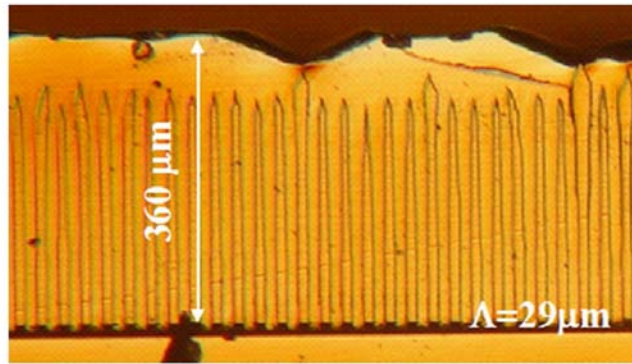


Figure 3. Early OPGaAs sample exhibiting domain degradation as growth proceeds up from template.

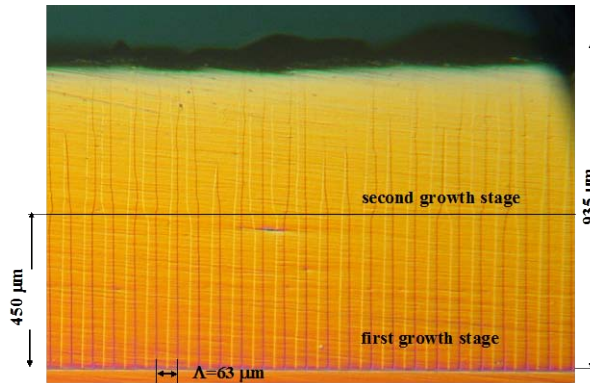


Figure 4. OPGaAs sample grown in two stages.

Parasitic growth arises because the supersaturation of the gas that drives rapid growth on the substrate also drives nucleation of GaAs on the quartz reactor walls; once such nucleation occurs there, the GaAs grows into large clusters that deplete the gas stream. Over the course of a long growth run (up to 10 hours), this so-called “parasitic” growth can severely diminish the rate of epitaxial wafer growth. Noting that previous attempts to grow orientation-patterned GaAs had occurred at atmospheric pressure, we developed a low-pressure process that would allow more efficient use of reactant gases at high velocity and high partial pressure. The first step was the construction of a custom-designed low-pressure HVPE reactor in which to grow 2-inch-diameter wafers. This fused-silica reactor, when sealed, permits operation of the HVPE system at a total pressure of 3.8 Torr. Its resistance-heated three-zone furnace provides the thermal environment for the gallium source zone, the mixing zone, and the deposition zone. A thermocouple probe

operating under the normal growth conditions calibrates the temperatures. With this system, growth rates over 180 microns per hour are readily achieved, producing total epilayer thicknesses of over 1.1 mm in a single 10 hour growth run.

Propagation of the desired pattern across the entire grown thickness was hindered by a tendency for overgrowth of the unpatterned regions into the patterned regions. This became especially noticeable on templates having many gratings separated by unpatterned “streets”, where the narrow gratings were easily overgrown from both sides. This effect can be reduced by minimizing unpatterned areas on the templates, or by using an “inverted” or “negative” template, in which the patterned regions have the orientation of the substrate, and the unpatterned regions have the inverted orientation (the reverse of the original template designs).

We have found that template design, growth regime, and surface morphology all strongly influence the vertical propagation of the domain walls, and it is beneficial to avoid conditions which promote faceting of the individual domains, as this tends to lead to loss of the initial grating periodicity. Due to this faceting behavior, the alignment of the initial grating with respect to the substrate miscut, typically 4° , is crucial for successfully maintaining the desired structure of $\{110\}$ -oriented antiphase boundaries. Such investigations have led to the growth OPGaAs with domains having an aspect ratio (width to height) of 1:25. A recent example of this sample quality is shown in Figure 5.

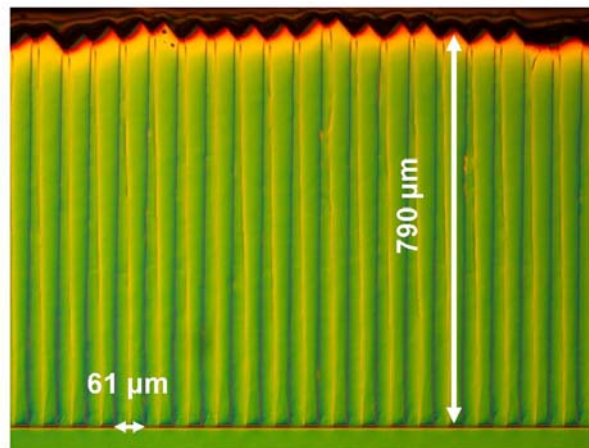


Figure 5. Recent OPGaAs sample with good domain fidelity across growth.

Optical losses, generally a combination of scattering and bulk material absorption, will decrease conversion efficiency, increase the OPO pumping threshold, and potentially lead to sample heating or even damage. Although OPGaAs samples don't have the kind of interface losses seen in the early diffusion-bonded stack samples, the domain boundaries are nonetheless interfaces, and may include defects that scatter or absorb the pump or output radiation. We have also determined that the mass flow rate of HCl gas strongly influences the free carrier concentration and with it, the amount of loss, such that control of this parameter has led to a significant increase in the transparency of HVPE-grown OPGaAs. Material is now routinely grown with optical loss below 0.01 cm^{-1} , which is the accuracy limit of linear, single-pass loss measurement techniques.

4. LOSS MEASUREMENT AND OPO PERFORMANCE

As mentioned above, reducing optical loss has been an important challenge in OPGaAs fabrication, and a necessary process for optimizing device performance. To understand the principal loss mechanisms more thoroughly, a detailed study was undertaken on an initial set of six OPGaAs samples. One sample was grown on a template from Stanford, and the rest were grown on templates from BAE Systems. Thick layer growth for all six was done at AFRL. Losses were measured at a wavelength of $2.05 \text{ }\mu\text{m}$, a typical pump wavelength for OPGaAs OPOs. The sample was placed in an

integrating sphere to allow determination of the relative contributions to overall loss of scatter and absorption, and the whole assembly was translated across the laser beam in fixed increments, providing a “map” of scatter, absorption, and overall loss across each sample.⁹

This study pointed to several general conclusions. First, scatter appeared to be the dominant loss mechanism in most cases, but there was no correlation between the type of loss mechanism and other characteristics such as distance from the substrate or periodicity of the grating. Loss varied significantly from sample to sample, and in most cases, across each sample. Overall loss was consistently higher in the patterned regions than in the unpatterned streets, and samples containing more than one period (multigrating samples) exhibited overall lower loss than those patterned with a single period. Material grown since this initial sample set has shown substantial improvement on all fronts. Not only is overall loss reduced, but uniformity and consistency have improved significantly, and the difference between loss in the patterned vs. unpatterned region is much less marked. This trend is certainly encouraging.

OPO performance was characterized using the experimental setup shown in Figure 6. The Tm,Ho:YLF pump laser operating at 2.05 μm was Q-switched at a repetition rate of 500 Hz, for a pulse width of 43 ns at an average output power of 1.5 W. The pump was focused to a radius (1/e²) of about 90 μm at the center of the OPGaAs sample, and attenuated to an average power of less than 150 mW to stay below the reported damage threshold of about 1.35 J/cm².⁴ The OPO resonator used meniscus mirrors with a 2.5-cm radius of curvature, coated for doubly resonant oscillation, with a reflectivity of 80% at the signal and idler wavelengths. The resonator was kept as short as possible to minimize threshold, and ranged from 1.2 cm to 2.0 cm depending on the sample length. For spectral analysis, the OPO output was directed into a monochromator with a cooled InSb detector.

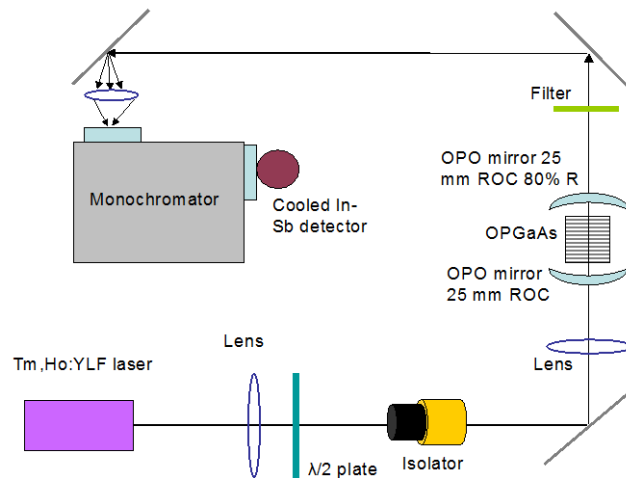


Figure 6. OPGaAs OPO Experiment.

After an initial set of measurements was completed, an etalon was inserted into the pump laser to study the effects on performance of reducing the pump laser linewidth. Although the original measured linewidth (without etalon) of 1.2 nm is well within the calculated phase-matching linewidth of 3.8 nm for this interaction in OPGaAs, further reduction of the linewidth was expected to improve efficiency by reducing the number of longitudinal modes in the pump output. With the etalon in place, the measured pump linewidth was 0.15 nm.

OPO pump threshold and slope efficiency results are summarized in Table 1 along with sample characteristics and previously measured loss data. Separate OPO measurements were made on each grating in the multigrating samples that produced sufficient stable output. The values listed represent the best location within each grating, and displacements of the beam from this location generally produced a marked reduction in output, in some cases even turning it off. Because of this variability, the minimum measured loss value was found to be a better indicator of OPO performance than the

average loss value. Several gratings suffered coating damage during the initial series of measurements, and thus could not be measured using the line-narrowed configuration. These are noted in the table as "damaged".

Our lowest threshold values are comparable to previously published results,⁴ and the higher values may be attributed at least in part to our use of an 80% R outcoupler, rather than the 90% R used in the referenced work. The previous results were also likely obtained using the best sample available, whereas we have investigated a broader range of samples in an effort to make comparisons among existing samples of OPGaAs material.

Table 1: OPGaAs OPO Performance Results.

Sample	Length (mm)	Period (μm)	Minimum Loss (1/cm)	Avg Loss (1/cm)	Without etalon		With etalon	
					% slope efficiency	Threshold (μJ)	% slope efficiency	Threshold (μJ)
4	10.3	62	1.2	0.054	4.2	95	damaged	
5	16.0	62	0.03	0.015	11.1	64	17.2	70
		63.8	0.03	0.005	10.3	122	damaged	
6	16.0	62	0.03	0.012	6.4	106	damaged	
		63	0.03	0.013	no output		no output	
7	17.0	61	0.86	0.033	4.5	67	14.3	88
		63	0.23	0.021	5.8	117	11.0	112
8	19.0	60.5	0.029*	0.093*	7.3	42	9.8	73
9	15.2	60.5	0.008*	0.03*	13.3	7	21.0	4

* Data provided by BAE Systems

Several noteworthy trends are evident from these data. First, slope efficiency is comparable for gratings on the same sample, and correlates roughly with minimum loss. This is consistent with the fact that material loss is strongly influenced by growth conditions, which will be fairly similar for all gratings on a given sample. Second, threshold is comparable for gratings having the same period, and increases with period size. We would expect instead for threshold to scale with loss, but the coatings on our resonator mirrors complicate matters. It turns out that the outcoupler reflectivity is close to 80% only from 3.6-4.9 μm; outside of this region, it decreases sharply. As the grating period increases, the signal and idler wavelengths move away from the 4.1 μm degeneracy point, and into these bands of lower reflectivity. Larger periods thus correspond to higher outcoupling "loss", and therefore increased threshold. This must be kept in mind as mirror coatings are specified.

It is also worth pointing out that samples 8 and 9 were the only samples produced in the same HVPE growth run, and the only samples grown with more than one template piece in the reactor. The two template pieces were placed at an angle in a "dish-rack" style holder, with sample 8 in front and sample 9 in back relative to the flow of reactants. Although sample 8 is significantly longer, sample 9 performed significantly better in the OPO. This highlights the difference in growth conditions experienced by each sample. Sample 8, encountering the reactants first, grew thicker, but both loss data and OPO results indicate that the quality of material in sample 9 is superior.

The wavelength of both signal and idler were measured separately for each grating. These are plotted in Figure 7 along with calculated tuning data based upon published refractive index measurements.¹⁰ The calculation is a good fit to the experimental data if a temperature of 305K is assumed, not unreasonable given that nothing was done to cool the samples or otherwise manage heat. The published refractive index data would seem, then, to be accurate, and the fabricated OPGaAs grating periods are very close to the intended design parameters.

Many additional samples have been grown since those measured here, and future experiments will compare their optical quality and OPO performance of some of these with that of the earlier material. Results obtained with this initial sample set already point to one reassuring conclusion: the BAE Systems templates yield device samples that are just as good as

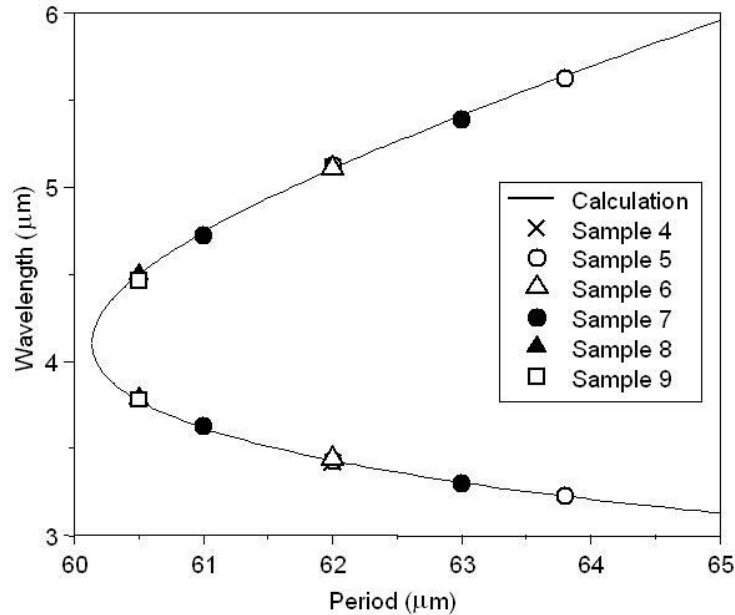


Figure 7. Calculated and experimental tuning data. (Note: data for 62 μm gratings on samples 4, 5, and 6 overlap.)

those grown on Stanford templates, validating the successful transition to industry of this important technology. Continued investigation is necessary before we can draw more meaningful correlations between OPO performance, optical loss characteristics, and material fabrication parameters. The experiments described here are intended to serve as a testbed for new samples as they become available.

5. FUTURE RESEARCH

Future research on OPGaAs will continue to focus on translating successful experimental results into reproducible, efficient, and useful devices. HVPE growth on bonded OPGaAs templates will allow the bonded template process to be refined to produce repeatable templates of a quality at least equivalent to those currently fabricated with a Ge layer. Bonded and other Ge-free template techniques are being explored in industry as well, which may ultimately result in the transition of more than one suitable process. Refinement of both template design and HVPE growth parameters will continue, with a goal of increasing sample thickness, domain fidelity, and optical quality to the point where CW operation of an OPO is possible.

Along with its many benefits, OPGaAs has one inescapable disadvantage: it cannot be pumped efficiently with a 1- μm pump source due to two-photon absorption, and thus cannot be paired with mature and readily available Nd and Yb lasers. Two-photon absorption occurs out to 1.7 μm , precluding the use of Er lasers in most conditions as well. For this reason, a critical component of future work is extending the OP technique beyond GaAs to materials with wider bandgaps in which these problems are not expected to occur. The two most promising candidates are GaP and ZnSe. These are listed in Table 2 along with OPGaAs and several other materials, including established nonlinear crystals like PPLN for comparison.

Table 2: Material comparisons¹¹

	GaAs	GaP	ZnSe	InAs	InP	ZGP	PPLN
d_{eff} (pm/V)	$> 90^3$	37	50	300	140	70	28
Transparency (μm)	1-16	0.6-11	0.5-22	3.8-7	1-14	0.7-11	0.35-4.5

GaP has a much lower nonlinear coefficient than GaAs, but is transparent down to 600 nm, allowing for pumping with a 1- μm laser as long as multiphonon processes remain negligible. Figure 8 compares the OPO tuning curves for OPGaAs and OPGaP at pump wavelengths of 1.5 μm and 2.05 μm , corresponding respectively to Er- and Ho-based lasers. The required domain widths (equal to the coherence length, or half the period) for a given interaction are longer in OPGaP than in OPGaAs, which tends to aid in preservation of the domain structure during thick-layer growth. The shallower slope of the dispersion curve in GaP translates into more relaxed acceptance bandwidths (spectral, thermal, input angle, etc.) in this material, and the multiple inflection points in the tuning curve suggest the prospect of generating two signal and idler pairs from the same grating period.

Several materials issues will need to be addressed before device-quality samples can be achieved, however. First, we must determine the extent to which material properties of epitaxially grown GaP differ from those of bulk GaP, for use in optimizing growth parameters and designing eventual devices. Also, two-photon absorption in GaP must be measured in order to verify appropriate pump laser wavelengths. The close lattice match between GaP and Si suggests the possibility of growing OPGaP on inexpensive and readily available Si substrates, but no templates have been produced by this method yet, and differences in the coefficients of thermal expansion between the two materials may lead to complications. When GaP templates are attempted, both substrate materials will merit investigation.

As CO₂ laser optics vendors have long appreciated, ZnSe has exceptionally broad transparency, with low linear absorption ($< 0.02 \text{ cm}^{-1}$)¹² and no two-photon absorption¹³ at wavelengths extending from less than 1 μm to 20 μm . As with GaP, the required domain widths for a given OPO interaction are wider in ZnSe than in GaAs, which makes the

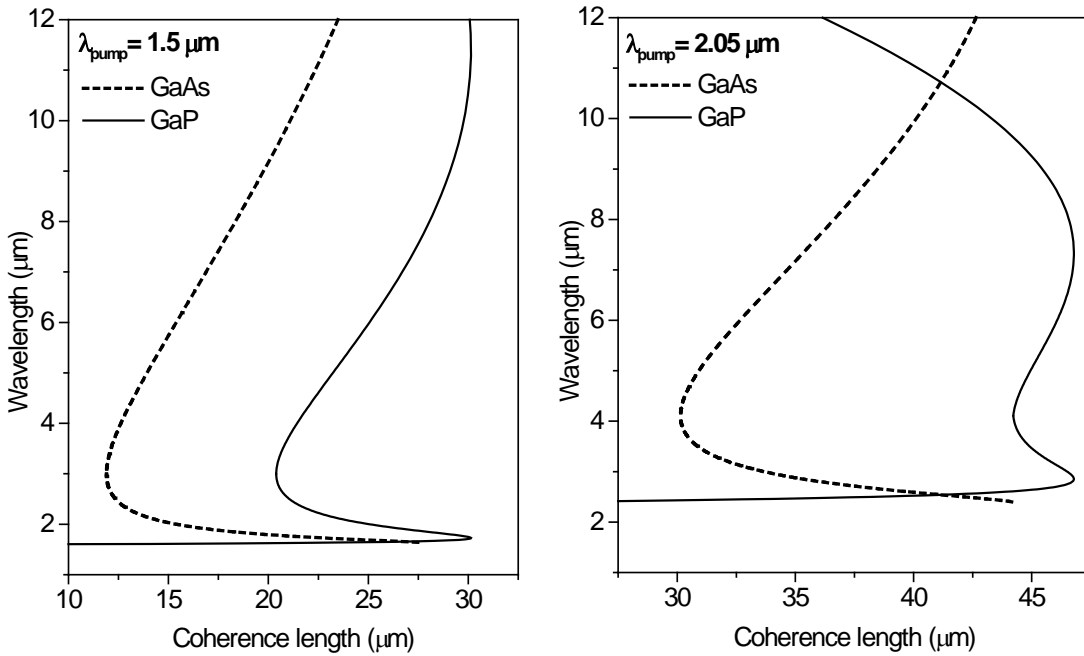


Figure 8. OPO Tuning curves for OPGaAs and OPGaP at pump wavelengths of 1.5 μm (left) and 2.05 μm (right).

growth of thick patterned films easier, and the shallower slopes of the dispersion curves lead to more relaxed acceptance bandwidths.

Growth of ZnSe is accomplished by first synthesizing a thin (few microns) layer in an evaporator chamber, and then using this film as a seed for thicker growth using physical vapor transport. Several years ago already up to 3 mm thickness have been achieved, with the first few hundred microns in single crystal form.¹⁴ The proof-of-concept in fabricating patterned ZnSe using a GaAs template has been demonstrated. The next step is fabrication of ZnSe devices of sufficient optical quality and size suitable for demonstration of frequency conversion.

6. CONCLUSION

Orientation patterned semiconductors constitute a third generation of nonlinear materials that are poised to provide frequency-converted laser sources in the 2-5 μm region as well as the 8-12 μm region for a variety of Air Force and commercial applications. Offering notable advantages over birefringently phase-matched crystals and poled ferroelectric materials, OP semiconductors exploit quasi-phases matching to produce a desired output wavelength while avoiding the intrinsic absorption, walkoff, and other problems of the earlier materials. Orientation-patterned GaAs-based devices have been fabricated to thicknesses of 1 mm and lengths of almost 30 mm, with losses below the measurement limit of 0.01 cm^{-1} , and a significant increase in both uniformity and repeatability. Optical loss and OPO performance measurements confirm the improvements in material quality, and provide useful insight into loss mechanisms, the relationship between growth conditions and device performance, and possible techniques for optimizing OP-semiconductor-based devices. Future work will focus on extending these techniques to materials beyond GaAs, and on transitioning successful methods into industrial processes capable of meeting Air Force and commercial needs.

Finally, we gratefully acknowledge Air Force Research Laboratory (AFRL), BAE Systems, and Northrop Grumman for funding support through CARMA; and AFRL Sensors and Materials Directorates and the Air Force Office of Scientific Research (AFOSR) for funding in-house OP semiconductor work. We also thank the following individuals for their technical contributions: K. Schepler, S. Lewis and G. Tietz (AFRL); J. Meyer and S. Shell (Air Force Institute of Technology); S. Setzler, T. Pollak, P. Schunemann, and L. Mohnkern (BAE Systems); N. B. Singh, A. Berghmans, and G. Kanner (Northrop-Grumman Corp.), and P. Kuo, X. Yu, M. Fejer, and S. Harris (Stanford University.)

REFERENCES

1. H. Schlossberg, A. Hordvik, A. Szilagy, "A quasi-phase-matching technique for efficient optical mixing and frequency doubling," *Journal of Applied Physics*, **v. 47**, pp. 2025-2032 (1976).
2. L. Gordon, G.L. Woods, R.C. Eckardt, R.R. Route, R.S. Feigelson, M.M Fejer, and R.L. Byer, "Diffusion-bonded stacked GaAs for Quasi-phase matched Second-Harmonic Generation of a Carbon Dioxide Laser," *Electronics Letters*, **v. 29**, pp. 1942-1944, (1993).
3. L. A. Eyres, P. J. Turreau, T. J.; Pinguet, C. B. Ebert, J. S. Harris, M. M. Fejer, L. Becouarn, B. Gerard, E. Lallier, "All-epitaxial fabrication of thick, orientation-patterned GaAs films for nonlinear optical frequency conversion," *Applied Physics Letters*, **v. 79**, p. 904 (2001).
4. P. G. Schunemann, S. D. Setzler, L. Mohnkern, T. M.; Pollak, D. F. Bliss, D. Weyburne, K. O'Hearn, "2.05- μm -laser-pumped orientation-patterned gallium arsenide (OPGaAs) OPO," *Conference on Lasers and Electro-Optics (CLEO)*, pp. 1835-1837 (2005).
5. K. L. Vodopyanov, O. Levi, P. S. Kuo, T. J. Pinguet, J. S. Harris, M. M. Fejer, B. Gerard, L. Becouarn, E. Lallier, "Optical parametric oscillation in quasi-phase-matched GaAs," *Optics Letters*, **v. 29**, pp. 1912-1914 (2004).
6. J. Li, D. B. Fenner, K. Temko, M. G.. Allen, P. F.. Moulton, C. Lynch, D. Bliss, W. D. Goodhue, "Wafer-fused orientation-patterned GaAs", Photonics West LASE 2008 Paper 6875-16.
7. T. J. Pinguet, O. Levi, T. Skauli, L. A. Eyres, L. Scaccabarozzi, M. M. Fejer, J. S. Harris, T. J. Kulp, S. Bisson, B. Gerard, L. Becouarn, E. Lallier, "Characterization of 0.5 mm thick films of orientation-patterned GaAs for nonlinear optical applications," *Conference on Lasers and Electro-Optics, Technical Digest*, p 138 (2001).
8. D.F. Bliss, C. Lynch, D. Weyburne, K. O'Hearn, and J.S. Bailey, *J. Crystal Growth* **287** (2006) 673-678.

9. Joshua W. Meyer, *Optical Characterization of Thick-Growth Orientation-Patterned GaAs*, Air Force Institute of Technology, Wright Patterson Air Force Base, OH (March 2006).
10. T. Skauli, P. S. Kuo, K. L. Vodopyanov, T. J. Pinguet, O. Levi, L. A. Eyres, J. S. Harris, M. M. Fejer, "Improved dispersion relations for GaAs and applications to nonlinear optics," *J Appl. Phys.* **v. 94**, pp. 6447-6455 (2003).
11. M. M. Fejer, "Orientation Patterned Semiconductors: Growth and Applications," unpublished briefing, Stanford University, 21 January 2004.
12. See visible-to-far infrared transmission spectrum of 1 cm length bulk ZnSe from II-VI website (<http://www.iiviiinfrared.com/materials.html#anchor2>) with $\alpha = 5 \times 10^{-4} \text{ cm}^{-1}$ at 10.6 μm .
13. J. Wang, M. Sheik-Bahae, A. A. Said, D. J. Hagan, and E. W. Van Stryland, "Time-resolved Z-scan measurements of optical nonlinearities," *J. Opt. Soc. Amer. B*, **v. 11**, pp. 1009-1017 (1994).
14. K. L. Schepler, D. F. Bliss, P. G. Schunemann, and G. Kanner, "Compact and Rugged Mid-Infrared Active Sensor" MSS Active E-O Systems Symposium (2004).